# *Natural Carbon By#Products for Transparent Heaters: The Case of Steam#Cracker Tar*

# Natural carbon by-products for transparent heaters: the case of steam-cracker tar

Owen P. Morris[1], Xining Zang[1], Aoife Gregg[1], Brent Keller[1], Bezawit Getachew[1], Samuel Ingersoll[1], Heather A. Elsen[2], Mark M. Disko[2], Nicola Ferralis[1], and Jeffrey C. Grossman*[1]

[1]Department of Materials Science and Engineering, Massachusetts Institute of Technology

[2]ExxonMobil Research and Engineering Co.



## Abstract

Steam cracker tar (SCT) is a byproduct of ethylene production which occurs in massive quantities globally (>150x10$^6$ tons/year). With few useful applications, the production of unwanted SCT leads to the need for its costly disposal or burning at the boiler plant. The discovery of new uses for SCT would therefore bring both economic and environmental benefits, although to date efforts towards employing SCT in diverse applications have been limited, and progress is further hampered by a lack of understanding of the material itself. Although complex and highly heterogeneous in nature, the molecular composition of SCT has the potential to serve as a diverse and tunable feedstock for wide-ranging applications. Here we report a simple solution processing method for SCT that allows its conductivity and optical properties to be controlled over orders of magnitude. By way of example, we focus here on the production of transparent conductive thin films, which exhibit a wide range of transparencies (23% to 93%) and sheet resistances (2.5Ω/□ to 1.2kΩ/□ ) that are tuned by a combination of solution concentration and thermal annealing. As transparent joule heaters, even without optimization these SCT devices show competitive performance compared to established technologies such as those based on reduced graphene oxide, and surpass the temperature stability limit of other materials. Furthermore, we demonstrate that laser annealing can be used to process



This is the author manuscript accepted for publication and has undergone full peer review but has not been through the copyediting, typesetting, pagination and proofreading process, which may lead to differences between this version and the Version of Record. Please cite this article as doi: 10.1002/adma.201900331

the SCT films and directly pattern transparent heaters on an arbitrary substrate. These results highlight the potential of SCT as a feedstock material for electronic applications and suggest that broader classes of either naturally occurring carbon or produced carbonaceous by-products could prove useful in a range of applications.

## Introduction

Natural carbons, such as coal and petroleum feedstocks, or the undesirable by-products of subsequent chemical processing of these feedstocks, such as tars, comprise a huge chemical phase space incorporating a wide range of chemical, optical and electronic properties. Most often these carbonaceous materials, whether from natural feedstock or industrial waste, are burned, with an associated generation of greenhouse gases.[1] Yet, given the chemical diversity in such materials it is of interest to explore their tunability and applicability in long-lifetime, potentially high-value products as opposed to single-use burning. For example, there is growing interest in extracting or synthesising graphene, carbon quantum dots, and other carbon nanomaterials from natural carbon, as they offer desirable electronic properties from inexpensive feedstocks, and recently thin films of coal microparticles were found to produce highly tunable electronic grade thin films.[2;3;4]

Steam cracker tar (SCT), a byproduct of the steam cracking process used to produce ethylene, has long been perceived as a material with few useful applications that is challenging to process.[5] The worldwide production of ethelyne exceeds that of any other organic compound, with 150 million tons produced in 2016 and demand forecast to rise to over 200 million tons by 2025.[6;7] The SCT, produced in large quantities, must then be removed or disposed of, at a cost to the producer or with corresponding emissions of greenhouse gases. SCT is a low value by-product, with its complex and diverse chemistry posing a barrier to its use as a synthesis feedstock.[8] As such, developing useful applications of SCT such as in optics or electronics would benefit both the producer and the environment.

SCT is a complex material primarily consisting of polycyclic aromatic hydrocarbons (PAHs) containing one to five rings, polymerized along a backbone similar to polystyrene when the aromatic residuals from the steam cracking process are quenched, and may also include unpolymerized PAHs

such as pyrene.[9] The exact composition of a SCT will depend on the specific feedstock used in the steam cracker. The SCT is cut with vacuum gas oil (VGO) to decrease its viscosity for transport away from the steam cracker - this mixture is known as fluxed SCT. The majority of the VGO is later distilled off, leaving a defluxed SCT.

Herein, we start from a defluxed SCT, and develop a solution processing method to produce highly uniform thin films of SCT and annealing procedures to produce transparent, more conductive films (see Figures. 1a-d). We characterize the optical and electronic properties of these films before and after annealing. Notably, we also demonstrate the first electronic device application for SCT by fabricating transparent Joule heaters, which can outperform more established materials such as reduced graphene oxide (rGO) and silver nanowires (AgNWs) in terms of maximum temperature, response time, ease of patterning, and materials costs.

## Results and Discussion

As received, highly viscous SCT was fully dissolved in dichloromethane (DCM), a solvent that has previously been used to dissolve both polystyrenes and various PAHs.[10] Thin films were prepared by spin-coating the solutions onto quartz disks. By varying the concentration of the SCT solution, we were able to easily vary the thickness of the final film over a range of hundreds of nanometers. SCT film thickness also depends on spin coating speed, where we choose 2000rpm unless otherwise noted. We then annealed these films in an argon atmosphere at a range of temperatures up to 950°C (it is important to note that this is significantly lower than the temperatures required to produce carbon black, which can be up to 2000°C).[11] As with conventional electronic-grade organic films, the SCT films are smooth and uniform over the whole sample, both before and after annealing, with example RMS roughnesses of 13nm and 11nm respectively (see cross sections in Figures. 1e and 1f, and representative profilometry in Figure S1). This represents a significant improvement over our previous work with films produced from ball-milled coal nanoparticles, where film performance was limited by the numerous cracks and voids present in the film after spin coating, which were then amplified by annealing[4].

When annealled, the SCT films lose large amounts of mass as shown by thermogravimetric

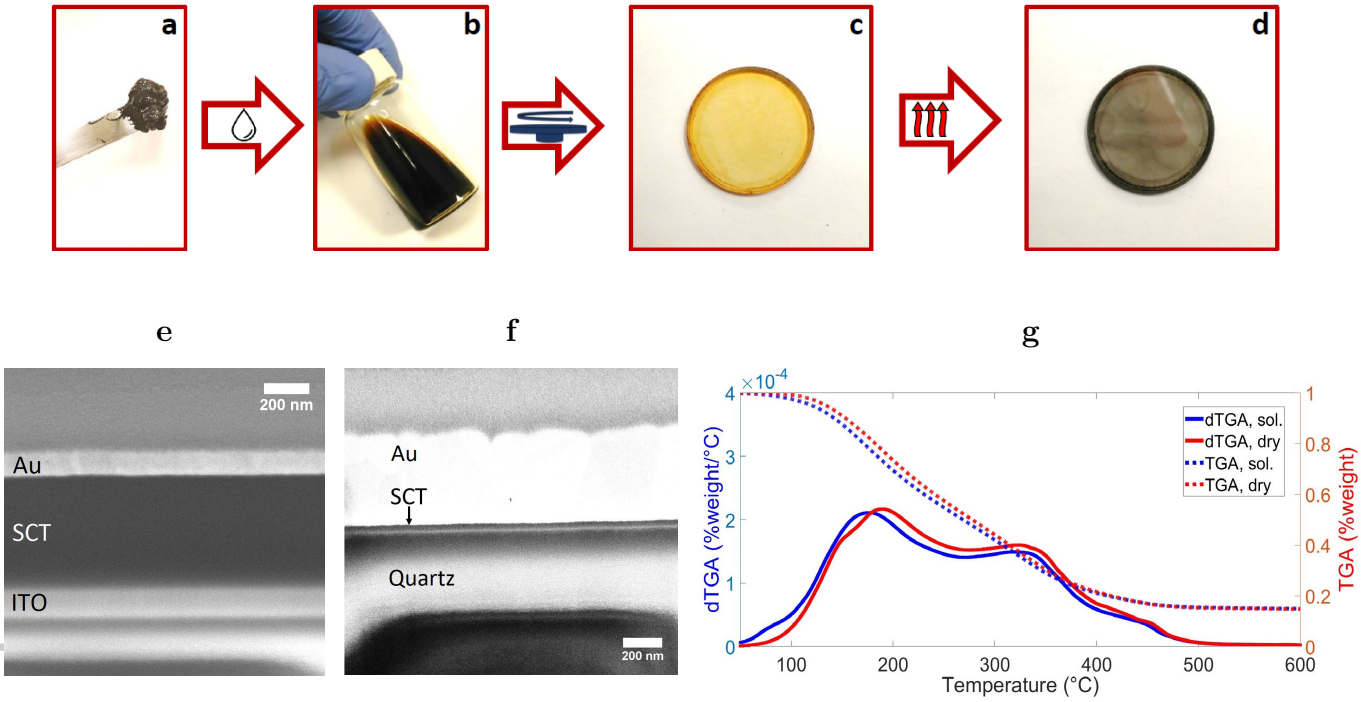


**Figure 1:** (a-d) Process flow for fabrication of thin SCT films. (a) High-viscosity defluxed SCT is (b) solvated in DCM or DCB. The resulting solution can be spin-coated onto a suitable substrate, resulting in a smooth homogeneous film (c), and is then annealed at high temperature, becoming thinner and darker (d). (e-f) Cross sectional images of (e) unannealed and (f) annealed SCT films. Au and ITO are used to improve the cross sections made via focused ion beam (FIB) milling and enhance the contrast of the SEM images. ITO was not included in the annealed device as it is not suitable for high temperature annealing. (g) TGA and dTGA of defluxed and solvated then dried SCT samples.

analysis (see Figure 1g), correlated with a large loss in film thickness, in some cases decreasing by as much as 95% (see Figures. 1e, 1f. Representative profilometry scans are included in Figure S1). To investigate this extreme mass loss and the composition of the SCT, we performed thermogravimetric analysis (TGA) up to temperatures as high as 950°C. Samples of defluxed SCT as received, as well as samples that were solvated in DCM and then dried for several days under vacuum, were tested.

The differential of the TGA scan (dTGA) shown in Figure 1g shows several features. Firstly, the two main peaks in the dTGA between 175-190°C and around 325°C likely correspond to the loss of the one- and two-ring aromatic molecules, respectively.[12;13;14] Expected percentages of core sizes in these SCT samples are roughly 35-50% one-ring and 35-55% two ring molecules, according to the SCT supplier, which fits well with the overall mass loss observed in the TGA. The smaller feature at 450°C could similarly be the loss of some or all of the three-ring cores. Secondly, the sample

that had been solvated then dried exhibits an extra shoulder between 60 and 100°C, showing that the spin coated films retain some solvent due to the high aromatic content of the SCT, which leads to high polarity regions of pi-pi molecular stacking that can trap polar solvent molecules like DCM, in a manner analagous to hydrogen bonding.[15] This must be heated to above the solvent boiling point to be removed, contributing to the mass loss upon annealing.

While the mass loss does not continue beyond 600°C (see extended TGA in Figure S2), the sheet resistances of films annealed at 600°C remain above 20kΩ/□, and therefore beyond the sensitivity of available characterization equipment. As we reported in our previous work on electronic devices made from various sintered coal particles, annealing between approximately 600 and 950°C causes a dramatic increase in carbon bond disorder and a rapid conversion to an aromatic-rich, highly interconnected a-C framework with significantly lower sheet resistance, with aromatic domain size increasing with temperature.[4] As expected, SCT films annealed at 950°C showed significantly lower sheet resistances, as low as around 1kΩ/□ depending on film thickness (see Figure 2c). This means that sheet resistance can be tuned both by annealing temperature and by coating parameters such as solution concentration.

The significant reduction in sheet resistance upon high temperature annealing derives from a change in the SCT chemical composition, which was quantified using UV-Vis absorption spectroscopy. UV-Vis absorption data is ideally suited to reveal details of the chemical structure of solid polyaromatic materials.[16] UV-Vis-NIR spectroscopy was performed in transmission mode to determine the optical transparency of the films before and after annealing, defined as the percentage transmittance at 550nm. Figure 2a shows the transmittance of SCT films with varying degrees of annealing. Two effects are competing here: the previously noted mass loss of the films up to 500-600°C, reducing the total light absorption; and the well known reduction of the bandgap with increasing conjugation at increasing annealing temperatures.[4;17;18] Figure 2a shows a dramatic decrease in the slope of the transmittance between unannealed films and those annealed at 400°C, indicating a decrease in bandgap according to the Tauc construction for disordered materials.[19] It is worth noting that slightly different treatments of the density of states and matrix elements result in different functional forms for the Tauc construction.[20] Here we have used the square root of the product of photon energy and absorbance, as it is generally considered appropriate for the

electronic states of a-C and hydrogenated amorphous carbon (a-C:H), and the good fit with our reported data gives us confidence in this treatment.[21] However, the absorption does not increase over the full spectral range due to the large mass loss reducing the film thickness. By 500°C, most of the mass loss has finished, but overall transmittance continues to decrease due to the lowering bandgap (see Figure 2b). This decrease continues to the films annealed at 950°C, with films coated from a solution of 100mg/ml decreasing to 23% transparency with thicknesses of tens of nanometers. However, since initial film thickness can be controlled via the solution concentration, films with transparencies as over 93% can be achieved even after annealing at 950°C.

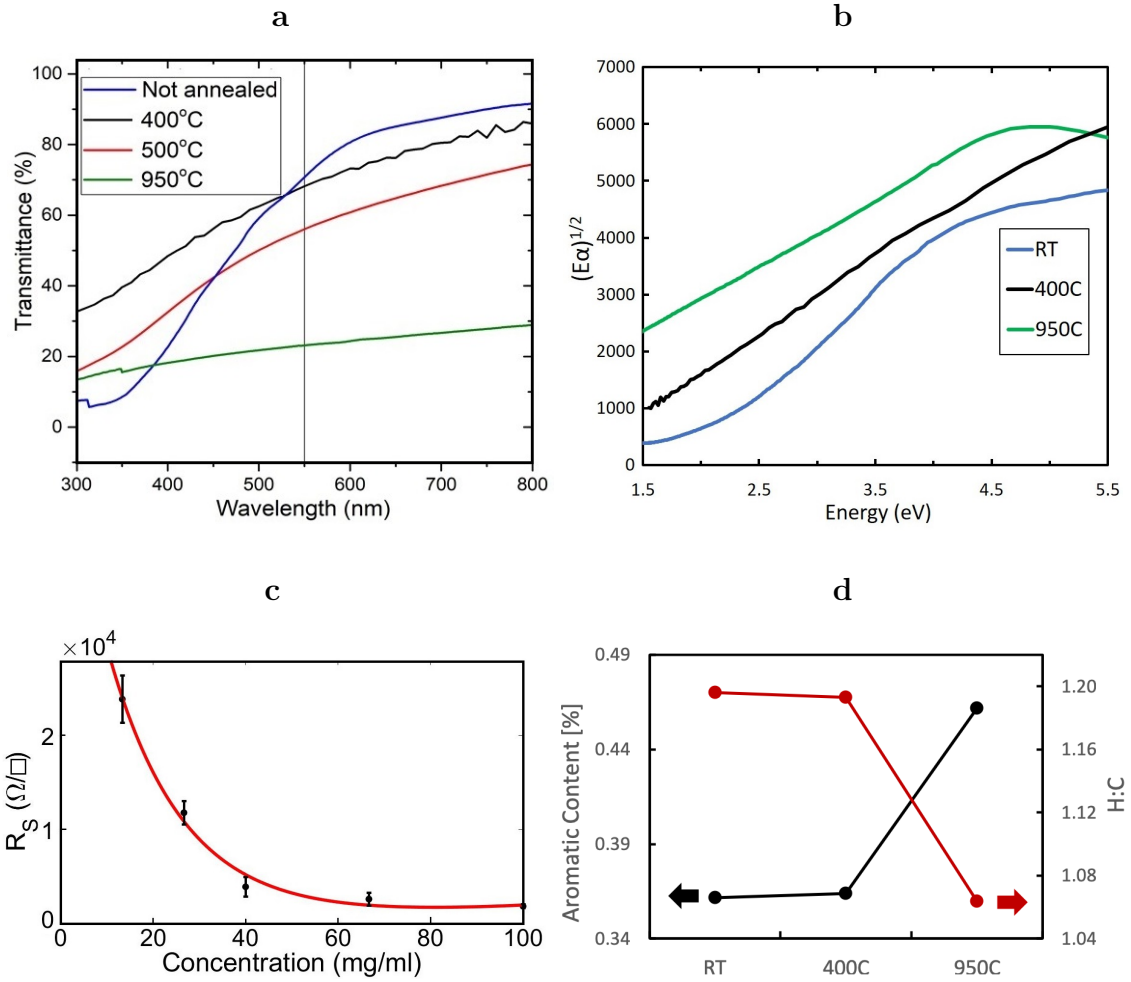


**Figure 2:** (a) Transmittance over a range of wavelengths for SCT films annealed at various temperatures. (b) Tauc construction used to fit bandgaps of SCT films annealed at various temperatures. (c) Sheet resistance after 950°C anneal as a function of initial solution concentration. (d) Aromatic content of films at various levels of annealing, obtained from Urbach tail energies derived from the films' visible absorption spectra following from [16].

Using the Urbach tail formalism, the exponential dependence of the absorption spectra to the inci-

dent wavelength is modulated by a characteristic decay width $E_0$.[22] The relations between $E_0$ and both H:C ratio and aromatic content are universal across different types of solid hydrocarbons.[16] It is worth noting that the both aromatic content and H:C ratio in solid hydrocarbons measured through the Urbach tail formalism correspond to the higher end of the distribution of aromatic sizes in the system, since the absorption spectrum is particularly sensitive to large clusters, such that $E_0$ should be correlated not with the average cluster size but instead to higher moments of the cluster size distribution.[16] Figure 2d shows the evolution of the aromatic content and H:C ratio of STC films from room temperature to 950°C. Minimal variations in either aromatic content or H:C ratios are observed at annealing at 450°C. Despite the significant mass loss of smaller aromatics and aliphatics in the as-prepared SCT film, the larger aromatics, which are those most prominently detected through UV-Vis absorption, are largely unchanged in size and in hydrogen content. We exclude the formation of any aromatic crosslinking at 450°C, since it would result in an increased averaged conjugation length and ultimately in a larger "apparent" aromatic core size.

Coal-based thin films proved to be excellent active materials for joule heaters, with high thermal resilience and stability while reaching sustained temperatures in excess of 300°C.[4] Having sheet resistances similar to those of much thicker coal-based films, while also being transparent, STC thin films are promising candidates for transparent heating, offering the strengths of coal based films with simpler processing, and the transparency required in applications such as de-icing aircraft or automobile windows, or for heating electronic devices such as LCD screens in cold environments.[23] The abundance of SCT as a byproduct makes it an attractive alternative to complex and costly materials such as nanowire networks or doped tin oxides, more mature transparent heating technologies.[23] Furthermore, silver nanowire (AgNW) films, a leading candidate in this field, tend to fail at temperatures above 120-200°C due to deteriorating connections between nanowires, and are synthesized from a high cost feedstock.[24;25]

In order to evaluate the potential of SCT films as transparent Joule heaters, we fabricated devices by sputtering metal contacts onto SCT films on quartz disks that had been annealled at 950°C. Device temperature was tracked in air under biases of up to 60V, resulting in temperatures as high as 279°C for less transparent films with transparencies of 23% - well above the temperature ceiling for many AgNW films - and the most transparent devices sustainted temperatures over 29°C, with

over 93% transparency (see Figures. 3c and 3d). Our devices thus span a wide potential application space, with higher transparency, lower temperature devices being suitable for autoglass or LCD screen de-icing, and higher temperature devices being useful for applications such as transparent supports for biomedical applications, where transparency is used for optical assessment of the active film, but high temperatures may be needed for sensor regeneration[26;27]. Furthermore, we performed extended heating tests in air with no observed drop in performance (see Figure S3a), highlighting that SCT devices are air stable over the whole range of temperatures, unlike comparable temperature transparent heaters that may require encapsulation.[28;29;30;31;32]

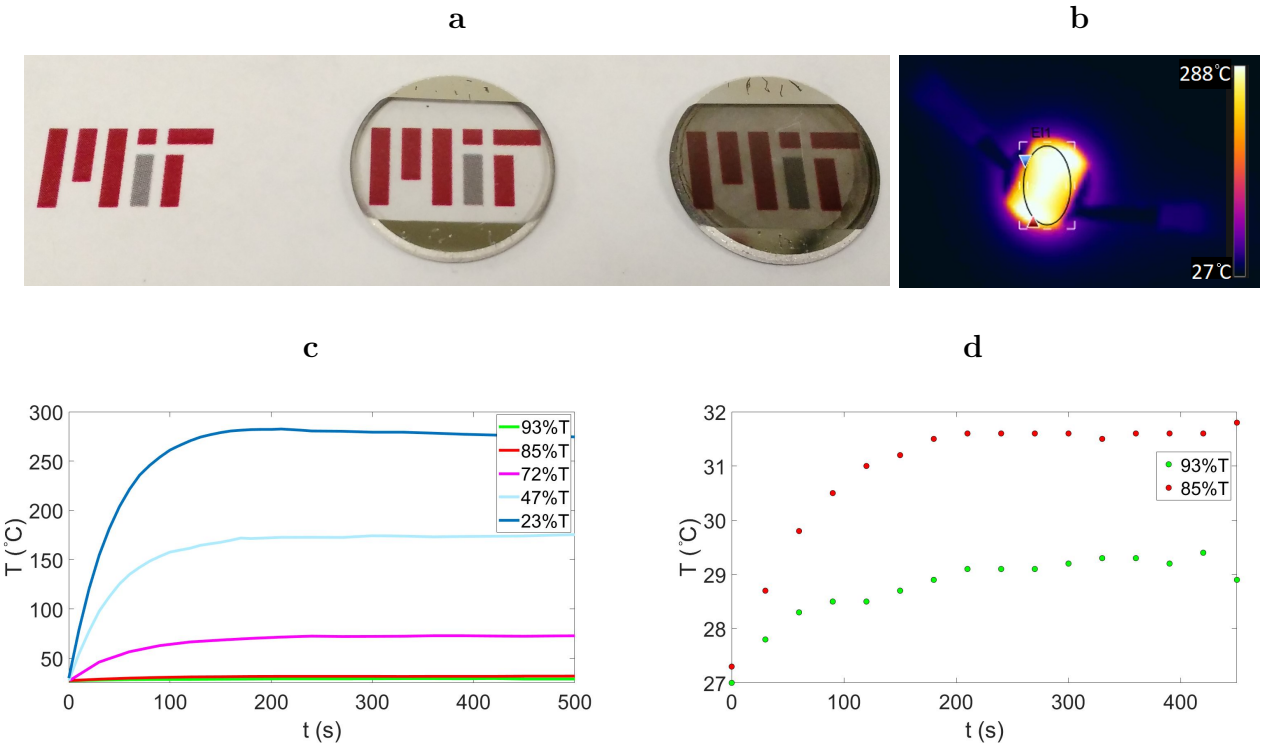


**Figure 3:** (a) Optical image of 94% and 23% transparent tar heaters over MIT logo. (b) SCT heater in operation during testing. (c) Heating responses under 60V bias of all heaters and (d) the two most transparent heaters.

For comparison with existing transparent heating technologies, we conducted a brief survey of the heating performance and transmission of devices in available literature, summarized in Figure 4. A full table with operating voltages and heating rates is included in Table S1. The United States federal government mandates a minimum of 70% light transmission through an automobile windshield, with lower resistances desirable when operating in fixed volatage modes for higher power output, where a minimum of 4.3J m$^{-}$2 is required for a thin film to remove the ice from a windshield.[33] The performance of our SCT devices spans the whole range of transparencies and

power outputs, and even unoptimized appear to be competitive with rGO devices operated under the same conditions, both at 60V , despite the fact that SCT is a low cost byproduct and available in industrial quantities, while commercial rGO costs a minimum of $50/g wholesale at time of writing (though we note that SCT films do exhibit slower heating rates).[34]

At lower temperatures, the performance of SCT devices lies below those of AgNW or polymer-based devices, which also are generally operated at lower voltages of 5-10V, but these devices lack stability at higher temperatures where SCT devices can still operate. Commercially SCT films offer numerous advantages, such as the potentially extremely low cost feedstock and the ability to make conformal, highly robust coatings just tens of nanometers thick from solution processing techniques. Furthermore, given the impressive stability at high temperatures of SCT, any future improvements in the electronic properties of the films would make SCT devices even more competitive. For example, reducing the resisitivity of the final films would improve both the maximum temperatures and heating rates, and could potentially be acheived via optimizations in processing or methods to increase the average aromatic cluster sizes.

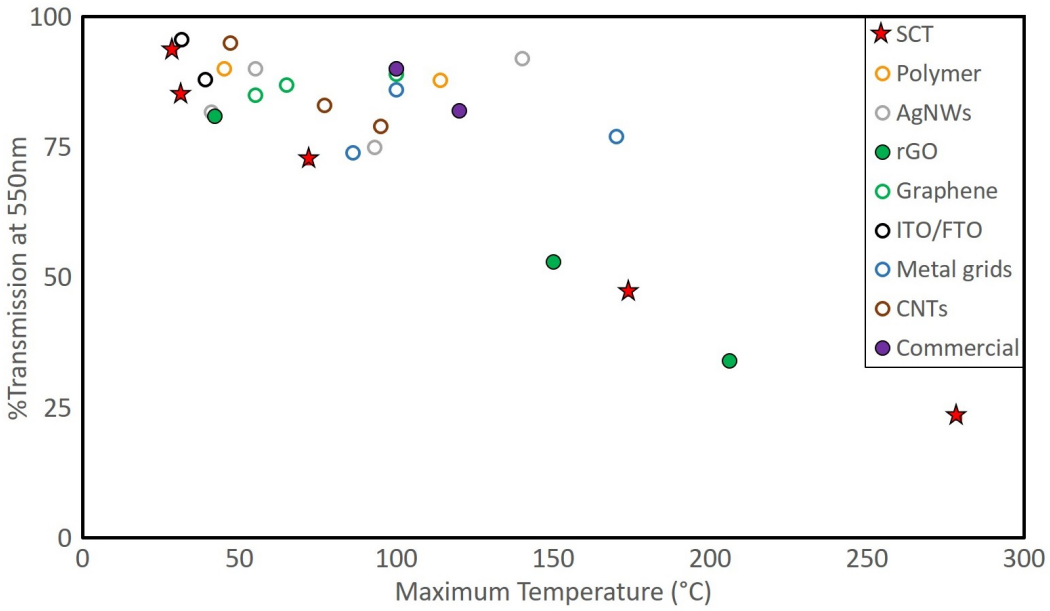


**Figure 4:** Performance comparison of various transparent heaters from literature and two commercial heating products, where higher maximum temperature (i.e. lower resistivity) and higher transmission are desirable. Unoptimized SCT devices from this work lie on a line of equal performance with rGO heaters. All references for the devices shown are listed in Table S1, along with heating rates and operating voltages.

As noted previously, SCT does contain a certain fraction of PAHs, some of which are listed as probable human carcinogens by the U.S. Environmental Protection Agency and more of which are currently not classifiable. While a full life cycle analysis of the material is beyond the scope of this paper, we do not believe that this would present a significant barrier to the commercialisation of SCT devices. While PAHs can be a health hazard in powder form or in soot given their potential to be aerosolized, SCT is an extremely viscous and inherently non-volatile liquid with no risk of exposure to its constituents. During processing, the PAHs are solvated and safe to use in normal lab or manufacturing conditions before deposition, and once deposited and annealed are bound to a substrate in a solid film, which our analysis of aromatic region size suggests is more graphitic in nature, with the PAHs in question fused into larger, non-volatile clusters.

Furnace annealed SCT films have uniform surfaces, which are essential for many electronic devices. However, the furnace size will limit the process sample size, which depending on the application can become a bottleneck for large scale manufacturing. Meanwhile, the strong absorption of SCT around 1000cm$^{-1}$ in its FTIR spectrum (see Figure 5a), inspired us to use a commercial laser cutter with a $CO_2$ laser (wavelength 10.6$\mu$m) as an alternate annealing method. Laser direct printing expands the processing opportunities for SCT films, and can shed light on their chemistry and further potential applications. The localized heating caused by the laser can be well in excess of the 950°C used in the furnace, but without the need for high temperature substrates, allowing potential applications on lower melting point and flexible substrates such as polyimide as with laser induced graphitization (LIG) films.[35;36]

Due to ablation of the film by the laser, thicker films are useful as a starting point. Drop cast films (from SCT dissolved in N-Methyl-2-pyrrolidone (NMP), with a concentration of 10 wt%) were ablated by a $CO_2$ laser cutter with a spot size of around 25$\mu$m. The laser pulse can generate up to 2600K locally with just 2W incident power on commercial polyimide tape.[35] The local high temperature enables carbonization of PAHs in SCT films in an ambient environment. Figure **??** shows drop-cast SCT films exposed to varying levels of projected laser power, where projected power is the percentage laser power divided by the percentage laser speed. Using a CAD interface, arbitrary patterns can be directly printed on and SCT film. While unannealed SCT is soluble in NMP, this is no longer true after annealing. The unexposed regions can then be washed away,

leaving a conductive pattern of annealed SCT as shown in Figure 5b. Figure 5c shows a preliminary example of a patterned heater in the shape of the MIT logo made with this method. This could make SCT films more useful for applications where the maximum visibility possible is desirable, as the minimum area necessary for heating can be patterned with an SCT heater and the remaining area left uncovered. It also increases the feasibility of large-scale manufacturing of SCT heaters, as laser patterning could be easily integrated on production lines.

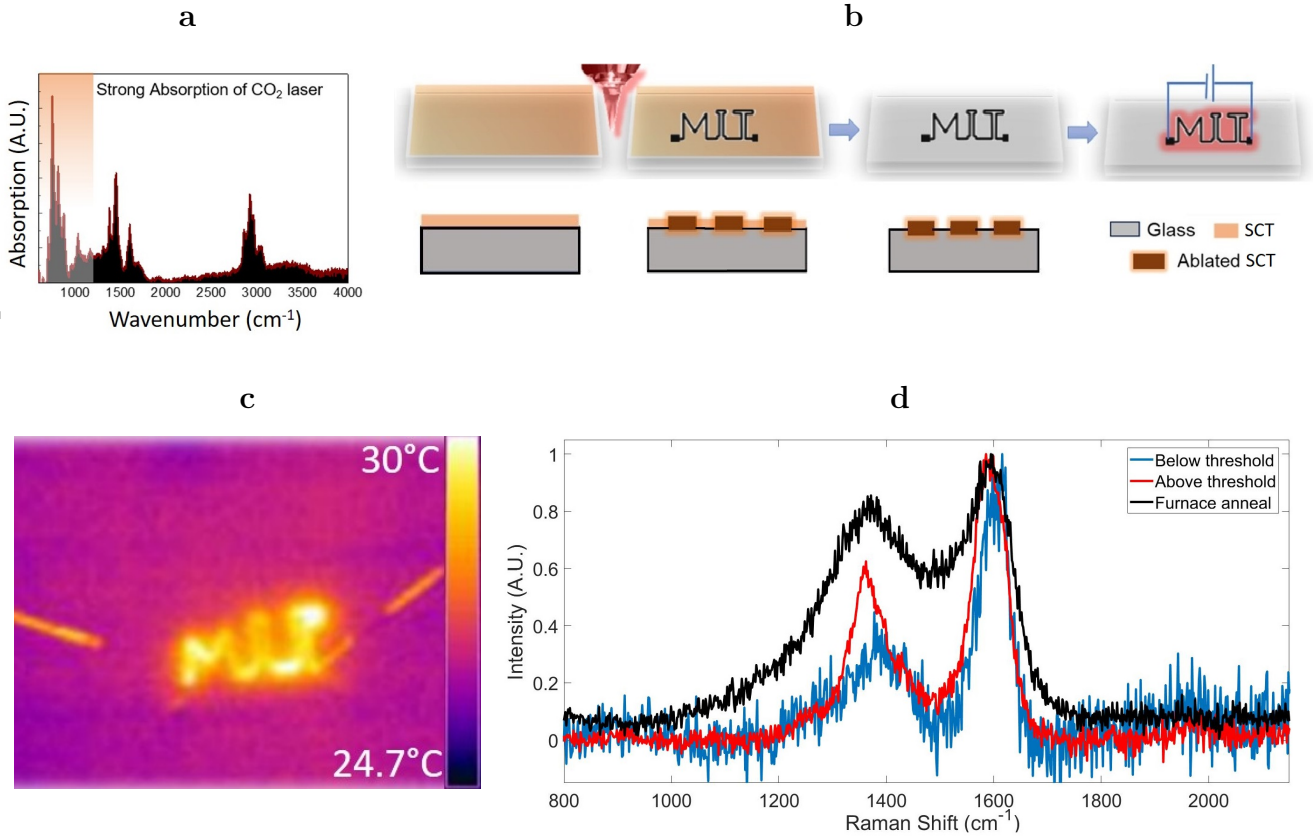


**Figure 5:** (a) FTIR absorption spectrum of SCT. (b) Direct write laser patterning process for SCT films. SCT films are annealed in a predefined pattern by a commercial laser cutter at low power, then washed with solvent to remove unannealed areas. (c) Patterned SCT heater featuring the MIT logo. (d) Raman spectra of SCT annealed via various methods.

The level of local annealing can be inferred from the ratio of the carbon D ($1350cm^{-1}$) and G ($1580cm^{-1}$) peak heights ($I_D/I_G$) in the Raman spectra, shown in Figure 5d, as this gives a measure of the aromaticity of the carbon.[37;38] The D peak is not found in either pure graphitic $sp^2$ or pure $sp^3$ carbon; thus, in a carbon sample containing finite size disordered $sp^2$ clusters, ($I_D/I_G$) will go through a maximum at some intermediate level of $sp^2$ ordering.[39] Strong fluorescence significantly overwhelms the raw Raman spectra for the as-prepared and low-temperature annealed

films, which is consistent with the unchanged nature of the aromatic cluster size, as fluorescence in aromatics is strongly related to the cluster size.[40] Annealing at 950°C, however, results in an increase in the size of the largest aromatic cores by roughly 25%, and a reduction in H:C by roughly 11% as previously shown. Fluorescence in Raman spectra is also reduced, consistent with more interconnected and larger aromatic cores. This increase in size and dehydrogenation leads to the lower sheet resistances observed. We predict that even higher annealing temperatures may lead to further reduction in sheet resistance, due to reduction of the bandgap with the extension of aromatic cores at increasing annealing temperatures.[4;17;18] Higher temperatures are also unlikely to lead to further mass loss given the trend originally observed in the TGA.

In SCT, it is clear that there is a threshold laser power below which no annealing occurs, after which ($I_D/I_G$) increases for increasing laser power, indicating improved annealing and likely increasing regions of disordered $sp^2$ clusters. Furthermore, above the power threshold a 2D peak appears (1350cm$^{-1}$), indicating graphitic ordering, shown in the expanded view in Figure S4. This is consistent with the production of LIG from commercial polymers shown by Lin et al.[35] However, laser annealed films never reach the maximum ($I_D/I_G$) achieved by furnace annealed films. Annealed and ablated SCT likely retain different types of defects such as oxygen, and as such ($I_D/I_G$) cannot be purely attributed to aromatic size. The sharper G peak of ablated SCT indicates a higher ordered graphitic concentration, while the smaller D peak implies a lower defect concentration. A full plot including more laser powers below and above the threshold can be found in Figure S4. The much faster heating kinetics of the laser source allow for rapid aromatic core size extension with minimal mass loss.

# Conclusions

We have demonstrated a new, solution-based processing method for SCT, a widely available and underutilized petrochemical by-product. By controlling solution concentrations and annealing temperatures, we were able to fabricate high quality thin films with a wide range of transparencies and sheet resistances. These films span the useful range of transparent heaters with temperatures up to 279°C and transparencies up to 93%. The heaters perform on par with synthentic rGO alternatives and show the potential to be competitive with existing technologies. Analysis of light absorption underscores the competition during annealing between mass loss, increase in aromatic core size, and aromatic connectivity, which can be decoupled from mass loss by using pulsed laser ablation. Furthermore, we demonstrate the feasibility of laser patterning the annealed sections of the films, creating patterned transparent heaters. From a broader standpoint, this research demonstrates the feasibility of petroleum byproducts as useful functional materials for optoelectronic technologies.

# Experimental Section

*Materials and chemicals:* Samples of defluxed SCT were obtained from ExxonMobil Research and Engineering Company. DCM ≥99.8% purity was purchased from Sigma Aldrich.

*Thin film synthesis:* SCT was dissolved in DCM in concentrations from 3.3-100mg $mL^{-1}$. Solutions of SCT in DCM were spin coated at 2000rpm for 20s onto quartz disks using a Laurell WS series spin coater. Annealing was performed in a quartz tube under argon flow for 30mins at a range of temperatures using a Lindberg/Blue $M^{TM}$ temperature controller. SCT dissolved in N-Methyl-2-pyrrolidone (NMP) with a concentration of 10wt% was drop cast onto glass slides and dried on a hot plate at 80°C to make a uniform thin film. Laser annealing was performed using a Universal Laser VLS 2.30 with a peak power output of 33W and percentage powers referenced to this value, with each pulse at sub-millisecond timescales and the scan speed set at 127mm $s^{-1}$.

*Characterisation:* Samples of defluxed SCT as received, as well as samples solvated in DCM and then dried for several days under vacuum, were tested using TGA up to 950°C. UV-Vis-NIR measurements were performed using a Perkin Elmer Lambda 1050 UV/VIS/NIR Spectrophotometer.

Film thicknesses were measured using a Bruker DXT Stylus Profilometer and cross sectional SEM performed on an FEI Helios 600. Sheet resistances were measured using a CDE ResMap 4-Point Probe. Temperature measurements were performed using Raman measurements were performed using a Horiba LabRam 800HR.

## Acknowledgements

This work was partially supported by ExxonMobil under the MIT Energy Initiative (Grant EM09079), and OM thanks the ExxonMobil Energy Fellow Program for partial support. This work made use of the MRSEC Shared Experimental Facilities at MIT, supported by the National Science Foundation under award number DMR-14-19807. Sheet resistance measurements and sputtering of electrodes were performed at the Center for Nanoscale Systems (CNS), a member of the National Nanotechnology Coordinated Infrastructure Network (NNCI), which is supported by the National Science Foundation under NSF award no. 1541959. CNS is part of Harvard University.

## Conflict of Interest

The authors declare no conflict of interest.

## Keywords

Natural carbon, petroleum by-product, transparent heater, solution processing, laser ablation.

# 1 Bibliography

[1] C. J. Yang. *Environ. Sci. Technol.* **2015**, *49*, 16 9501.

[2] R. Ye, C. Xiang, J. Lin, Z. Peng, K. Huang, Z. Yan, N. P. Cook, E. L. G. Samuel, C.-c. Hwang, G. Ruan, G. Ceriotti, A.-r. O. Raji, J. M. Tour, A. A. Martı. *Nat. Commun.* **2013**, *4*, 2943 1.

[3] R. Kumar, R. Kumar, D. Pratap. *Renew. Sustain. Energy Rev.* **2016**, *58* 976.

[4] B. D. Keller, N. Ferralis, C. Grossman. *Nano Letters* **2016**, *16* 2951.

[5] J. N. McCoy, P. F. Keusenkothen. *US Patent* **2008**, US20080116109A1.

[6] Market Publishers. The Ethylene Technology Report 2016, **2016**.

[7] Wood Mackensie Chemicals. Ethylene Global Supply Demand Analytics Service - April 2018, **2018**.

[8] T. Kan, X. Sun, H. Wang, C. Li, U. Muhammad. *Energy & Fuels* **2012**, *26*, 6 3604.

[9] P. R. Solomon, H. H. King. *Fuel* **1984**, *63*, 9 1302.

[10] W. Wang, B. Meng, X. Lu, Y. Liu, S. Tao. *Anal. Chim. Acta* **2007**, *602*, 2 211.

[11] Kuhner, G.; Manfred, V. *Carbon Black Science and Technology.* CRC Press, **1993**.

[12] V. Oja, E. M. Suuberg. *ACS Div. Fuel Chem. Prepr.* **1996**, *41*, 1 82.

[13] M. D. Guillén, A. Domínguez, M. J. Iglesias, E. Fuente, C. G. Blanco. *Fuel* **1996**, *75*, 9 1101.

[14] V. Risoul, C. Pichon, G. Trouvé, W. A. Peters, P. Gilot, G. Prado. *J. Hazard. Mater.* **1999**, *64*, 3 295.

[15] M. Nishio. *Phys. Chem. Chem. Phys.* **2011**, *13*, 31 13873.

[16] N. Ferralis, Y. Liu, K. D. Bake, A. E. Pomerantz, J. C. Grossman. *Carbon* **2015**, *88* 139.

[17] J. Robertson, E. O'Reilly. *Physical Review B* **1987**, *35*, 6 2946.

[18] J. Robertson. *Progress in Solid State Chemistry* **1991**, *21*, 4 199.

[19] J. Tauc, R. Grigorovici, A. Vancu. *Phys. Status Solidi* **1966**, *15* 627.

[20] E. A. Davis, N. F. Mott. *Philos. Mag. A J. Theor. Exp. Appl. Phys.* **1970**, *22*, 179 0903.

[21] J. Robertson. *Adv. Phys.* **1986**, *35*, 4 317.

[22] Y. Ruiz-Morales, X. Wu, O. C. Mullins. *Energy and Fuels* **2007**, *21*, 2 944.

[23] R. Gupta, K. D. Rao, S. Kiruthika, G. U. Kulkarni. *ACS Applied Materials and Interfaces* **2016**, *8*, 20 12559.

[24] D. C. Choo, T. W. Kim. *Sci. Rep.* **2017**, *7*, 1 1.

[25] P. H. Wang, S. P. Chen, C. H. Su, Y. C. Liao. *RSC Adv.* **2015**, *5*, 119 98412.

[26] J. A. Goode, J. V. H. Rushworth, P. A. Millner. *Langmuir* **2015**, *31*, 23 6267.

[27] S. Leahy, Y. Lai. *Sensing and Bio-Sensing Research* **2015**, *6* 25.

[28] M. N. Gueye, A. Carella, R. Demadrille, J. P. Simonato. *ACS Appl. Mater. Interfaces* **2017**, *9*, 32 27250.

[29] J. Kang, H. Kim, K. S. Kim, S. K. Lee, S. Bae, J. H. Ahn, Y. J. Kim, J. B. Choi, B. H. Hong. *Nano Lett.* **2011**, *11*, 12 5154.

[30] L. Zhang, Y. Chen, C. Xu, Z. Liu, Y. Qiu. *RSC Adv.* **2018**, *8*, 26 14532.

[31] H. Zhai, R. Wang, X. Wang, Y. Cheng, L. Shi, J. Sun. *Nano Res.* **2016**, *9*, 12 3924.

[32] Q. Huang, W. Shen, X. Fang, G. Chen, J. Guo, W. Xu, R. Tan, W. Song. *RSC Adv.* **2015**, *5*, 57 45836.

[33] S. W. L. Shames, C. M. Zhang, N. Ferralis, J. C. Grossman. *International Journal of Energy Efficient Vehicle Designs* **2013**, *15*, 2 1114.

[34] Shandong Runyi Chemical Co., Ltd. Reduced graphene oxide powder, wholesale. `https://www.alibaba.com/product-detail/Reduced-graphene-oxide-powder_60867572052.html?spm=a2700.7724857.normalList.16.1666486326dL0I`. Accessed: 2019-03-16.

[35] J. Lin, Z. Peng, Y. Liu, F. Ruiz-zepeda, R. Ye, E. L. G. Samuel, M. J. Yacaman, B. I. Yakobson, J. M. Tour. *Nat. Commun.* **2014**, *5* 1.

[36] R. Ye, D. K. James, J. M. Tour. *Acc. Chem. Res.* **2018**, *51*, 7 1609.

[37] A. C. Ferrari, J. Robertson. *Phys. Rev. B* **2000**, *61*, 20 95.

[38] A. C. Ferrari, J. Robertson. *Phys. Rev. B - Condens. Matter Mater. Phys.* **2001**, *64*, 7 1.

[39] J. Schwan, S. Ulrich, V. Batori, H. Ehrhardt, S. R. P. Silva. *J. Appl. Phys.* **1996**, *80*, 120 1611.

[40] Y. Liu, N. Ferralis, L. T. Bryndzia, J. C. Grossman. *Carbon* **2016**, *101* 361.

[41] C. Celle, C. Mayousse, E. Moreau, H. Basti, A. Carella, J. P. Simonato. *Nano Res.* **2012**, *5*, 6 427.

[42] S. Wang, X. Zhang, W. Zhao. *J. Nanomater.* **2013**, *2013*, 3 1.

[43] X. He, R. He, Q. Lan, W. Wu, F. Duan, J. Xiao, M. Zhang, Q. Zeng, J. Wu, J. Liu. *Materials (Basel).* **2017**, *10*, 3.

[44] J. Li, J. Liang, X. Jian, W. Hu, J. Li, Q. Pei. *Macromolecular Materials and Engineering* **2014**, *299*, 11 1403.

[45] D. Sui, Y. Huang, L. Huang, J. Liang, Y. Ma, Y. Chen. *Small* **2011**, *7*, 22 3186.

[46] B. J. Lee, G. H. Jeong. *Curr. Appl. Phys.* **2012**, *12*, 4 113.

[47] H. S. Jang, S. K. Jeon, S. H. Nahm. *Carbon N. Y.* **2011**, *49*, 1 111.

[48] Y. H. Yoon, J. W. Song, D. Kim, J. Kim, J. K. Park, S. K. Oh, C. S. Han. *Adv. Mater.* **2007**, *19*, 23 4284.

[49] T. J. Kang, T. Kim, S. M. Seo, Y. J. Park, Y. H. Kim. *Carbon N. Y.* **2011**, *49*, 4 1087.

[50] C. Hudaya, J. H. Park, W. Choi, J. K. Lee. *ECS Trans.* **2013**, *53*, 4 161.

[51] S. Kiruthika, R. Gupta, G. U. Kulkarni. *RSC Adv.* **2014**, *4*, 91 49745.

[52] R. Gupta, K. D. Rao, K. Srivastava, A. Kumar, S. Kiruthika, G. U. Kulkarni. *ACS Appl. Mater. Interfaces* **2014**, *6*, 16 13688.

[53] D. Lordan, M. Burke, M. Manning, A. Martin, A. Amann, D. O'Connell, R. Murphy, C. Lyons, A. J. Quinn. *ACS Appl. Mater. Interfaces* **2017**, *9*, 5 4932.

[54] T. Kim, Y. W. Kim, H. S. Lee, H. Kim, W. S. Yang, K. S. Suh. *Adv. Funct. Mater.* **2013**, *23* 1250.

[55] Minco. Thermal-Clear™ transparent heaters. `https://www.minco.com/~/media/files/minco/productguides/heat/`. Accessed: 2019-03-19.

[56] Transparent Products, Inc. CrystalHeat® LCD heaters. `https://www.touchpage.com/wp-content/uploads/2018/12/CrystalHeat_Datasheet.pdf`. Accessed: 2019-03-19.

# Supporting Information

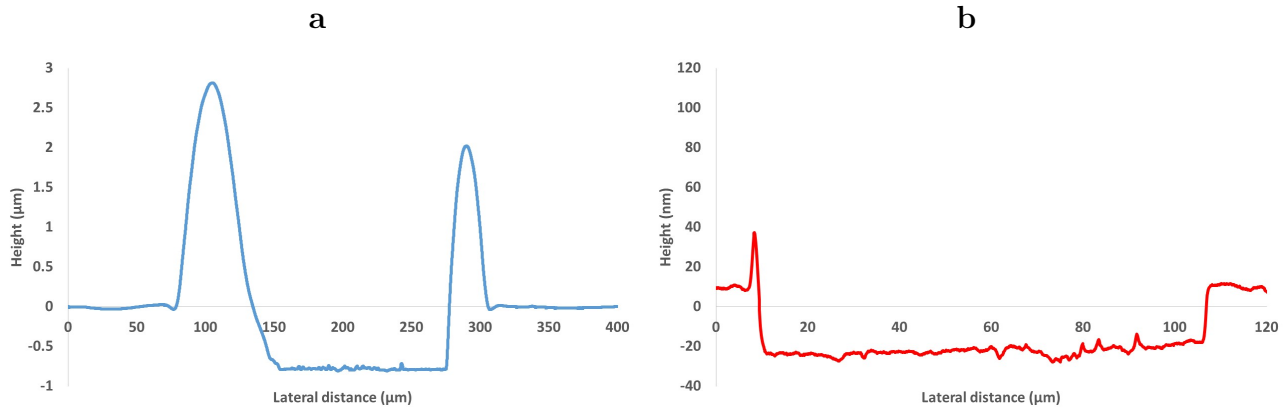


**Figure S1:** Profilometry line scans showing the thicknesses of sample (a) unannealed and (b) 950°C furnace annealed SCT.

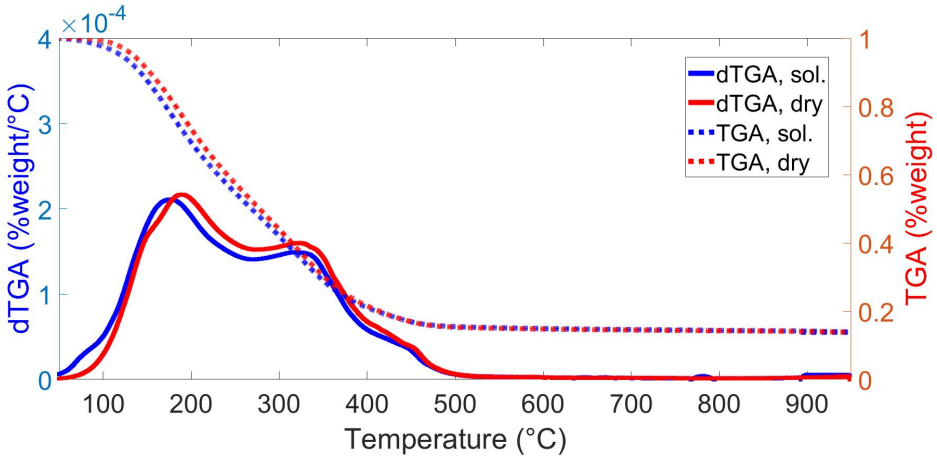


**Figure S2:** Extended SCT TGA scan.

| Material | %T | Max T [°C] | Voltage [V] | Rate [°C $s^{-1}$] | ΔT/ΔV [°C $V^{-1}$] | Ref. |
|---|---|---|---|---|---|---|
| AgNWs | 81.8 | 41 | 5 | 1.5 | 3.2 | [39] |
| AgNWs | 92 | 140 | 7 | 0.8 | 16.4 | [40] |
| AgNWs | 90 | 55 | 7 | 2.0 | 4.3 | [39] |
| AgNWs | 75 | 93 | 4 | 0.2 | 17.0 | [25] |
| AgNWs | 90 | 100 | 7 | 1.3 | 10.7 | [52] |
| Composite | 74.1 | 99 | 40 | 1.1 | 1.9 | [41] |
| Composite | 86.4 | 230 | 13 | *Not reported* | 15.8 | [42] |
| rGO | 34 | 206 | 60 | 7.0 | 3.0 | [43] |
| rGO | 53 | 150 | 60 | 7.0 | 2.1 | [43] |
| rGO | 81 | 42 | 60 | 0.7 | 0.3 | [43] |
| Graphene | 89 | 100 | 12 | 0.8 | 6.3 | [27] |
| Graphene | 87 | 65 | 12 | 0.5 | 3.3 | [27] |
| Graphene | 85 | 55 | 40 | 0.3 | 0.8 | [44] |
| CNTs | 83 | 77 | 15 | *Not reported* | 3.5 | [45] |
| CNTs | 79 | 95 | 12 | 0.9 | 5.8 | [46] |
| CNTs | 95 | 47 | 60 | 0.4 | 0.4 | [47] |
| ITO | 95.6 | 31.4 | 12 | 0.1 | 0.5 | [27] |
| FTO | 88 | 39 | 12 | 0.0 | 1.2 | [48] |
| Metal Grid | 77 | 170 | 8.5 | 1.2 | 17.1 | [49] |
| Metal Grid | 86 | 100 | 5 | 1.9 | 15.0 | [50] |
| Metal Grid | 74 | 86 | 5 | 3.1 | 12.2 | [51] |
| Polymer | 87.8 | 114 | 10 | 1.2 | 8.9 | [26] |
| Polymer | 90.1 | 45 | 10 | 0.2 | 2.0 | [26] |
| Commercial (Composite) | 82 | 120 | *Not available* | *Not available* | *Not available* | [53] |
| Commercial (ITO) | 90 | 100 | *Not available* | *Not available* | *Not available* | [54] |
| Coal | 25 | 285 | 60 | 2.2 | 4.3 | [4] |
| SCT | 23.1 | 279.3 | 60 | 4.2 | 4.2 | This work |
| SCT | 46.9 | 174.2 | 60 | 2.5 | 2.5 | This work |
| SCT | 72.2 | 72.1 | 60 | 0.8 | 0.8 | This work |
| SCT | 84.7 | 31.6 | 60 | 0.1 | 0.1 | This work |
| SCT | 93.3 | 29.2 | 60 | 0.1 | 0.1 | This work |

**Table S1:** Performance comparison of various transparent heaters from literature and two commercial heaters.

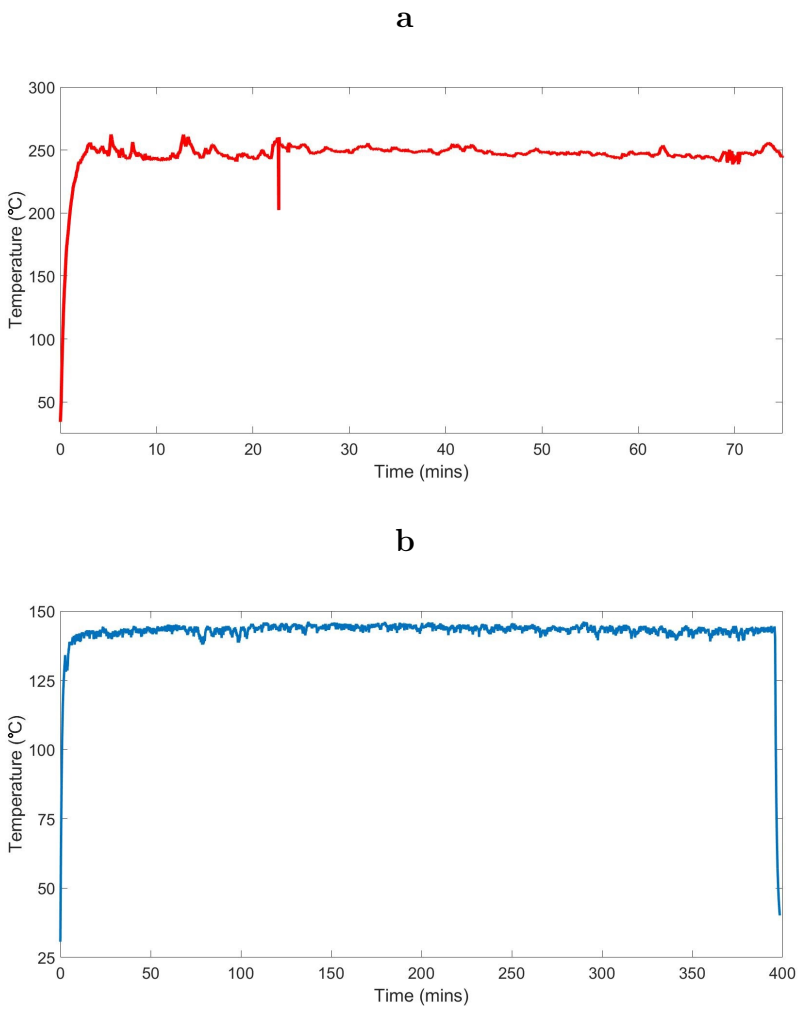


**Figure S3:** Extended air stability tests for (a) a high temperature resistive heater and (b) an intermediate temperature heater. Sharp fluctuations are due to instabilities in the supplied voltage. Sharp decline at the end of (b) from voltage suply being turned off.

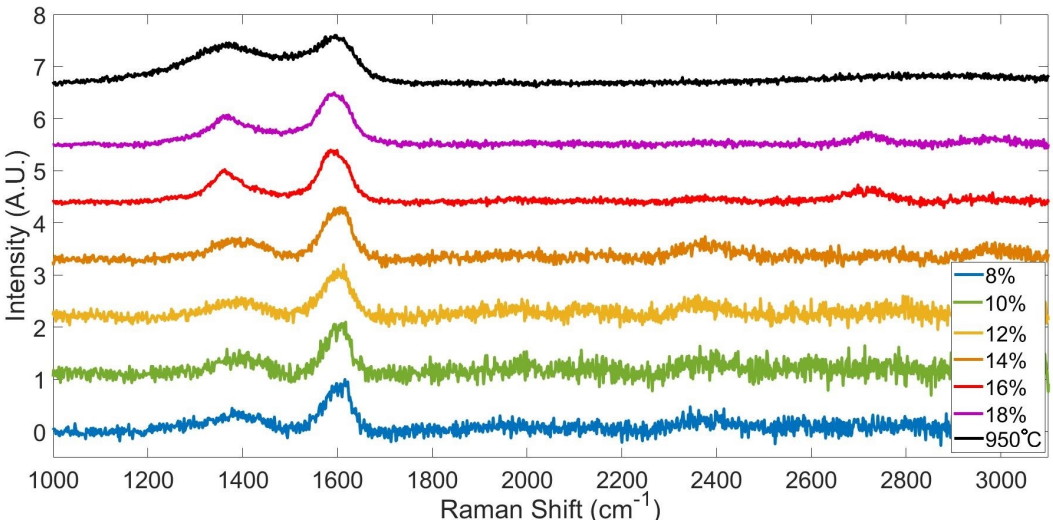


**Figure S4:** Raman spectra for annealing done with various percentage laser powers and with a 950°C furnace anneal.